Translational Oncology
www.transonc.com

Volume 7 Number 2 April 2014 pp. 309–321 309

Hippo Signaling Mediates Proliferation, Invasiveness, and Metastatic Potential of Clear Cell Renal Cell Carcinoma[1]

Ute Schütte*, Savita Bisht*, Lukas C. Heukamp†, Moritz Kebschull‡, Alexandra Florin†, Jens Haarmann*, Per Hoffmann§,¶,#, Gerd Bendas, Reinhard Buettner†, Peter Brossart* and Georg Feldmann***

*Department of Internal Medicine 3, Center of Integrated Oncology Cologne-Bonn, University Hospital of Bonn, Bonn, Germany; †Institute of Pathology, Center of Integrated Oncology Cologne-Bonn, University Hospital of Cologne, Cologne, Germany; ‡Department of Periodontology, Operative and Preventive Dentistry, University Hospital of Bonn, Bonn, Germany; §Institute of Human Genetics, University Hospital of Bonn, Bonn, Germany; ¶Department of Genomics, Life and Brain Center, University Hospital of Bonn, Bonn, Germany; #Division of Medical Genetics, University Hospital and Department of Biomedicine, University of Basel, Basel, Switzerland;**Department of Pharmacy, University of Bonn, Bonn, Germany

Abstract

Recent work has identified dysfunctional Hippo signaling to be involved in maintenance and progression of various human cancers, although data on clear cell renal cell carcinoma (ccRCC) have been limited. Here, we provide evidence implicating aberrant Hippo signaling in ccRCC proliferation, invasiveness, and metastatic potential. Nuclear overexpression of the Hippo target Yes-associated protein (YAP) was found in a subset of patients with ccRCC. Immunostaining was particularly prominent at the tumor margins and highlighted neoplastic cells invading the tumor-adjacent stroma. Short hairpin RNA-mediated knockdown of YAP significantly inhibited proliferation, migration, and anchorage-independent growth of ccRCC cells in soft agar and led to significantly reduced murine xenograft growth. Microarray analysis of YAP knockdown *versus* mock-transduced ccRCC cells revealed down-regulation of endothelin 1, endothelin 2, cysteine-rich, angiogenic inducer, 61 (CYR61), and c-Myc in ccRCC cells as well as up-regulation of the cell adhesion molecule cadherin 6. Signaling pathway impact analysis revealed activation of the p53 signaling and cell cycle pathways as well as inhibition of mitogen-activated protein kinase signaling on YAP down-regulation. Our data suggest CYR61 and c-Myc as well as signaling through the endothelin axis as *bona fide* downstream effectors of YAP and establish aberrant Hippo signaling as a potential therapeutic target in ccRCC.

Translational Oncology (2014) 7, 309–321

Introduction

Renal cell carcinoma (RCC) accounts for about 2% to 3% of all malignant diseases in adults with clear cell RCC (ccRCC) being the most common histologic subtype that represents 70% to 80% of all cases [1]. Despite the emergence of novel targeted therapies such as antiangiogenetic drugs and mammalian target of rapamycin inhibitors over the last decade, the prognosis of metastatic renal cancer remains poor with 5-year survival rates of less than 10% [2]. This grim prognosis poses the need for a better understanding of the underlying molecular mechanisms driving metastatic ccRCC to be able to develop novel therapeutic approaches.

Address all correspondence to: Georg Feldmann, MD, Department of Internal Medicine 3, Center of Integrated Oncology Cologne-Bonn, University Hospital of Bonn, Biomedizinisches Zentrum, Room 3G 024, Sigmund-Freud-Str. 25, D-53127 Bonn, Germany. E-mail: georg.feldmann@uni-bonn.de

[1] This work was supported in part by the German Cancer Foundation (Deutsche Krebshilfe) under grants 109215 and 109929 and by the European Community's Seventh Framework Program (FP7-2007-2013) under grant agreement HEALTH-F2-2011-256986. S.B. was supported by BONFOR grant O-142.0005.
Received 4 September 2013; Revised 3 February 2014; Accepted 4 February 2014

1936-5233/14 http://dx.doi.org/10.1016/j.tranon.2014.02.005

The Hippo signaling pathway has been found to be evolutionary conserved and to function as a critical regulator of organ size control. Moreover, we and others have recently been able to show that Hippo signaling exerts a dramatic oncogenic potential in several human malignancies [3,4]. Although germ-line and somatic mutations of the Hippo pathway core components are rare, deregulation and subsequent overexpression of Yes-associated protein (YAP) have been observed in many human cancers [5-7]. However, as of to date, little data exist on the role of Hippo signaling in ccRCC.

In this study, we demonstrate that Hippo signaling is activated in ccRCC and is involved in regulating proliferation, invasiveness, and metastatic potential. Downstream effectors of Hippo signaling in ccRCC are characterized to identify potential targets for therapeutic intervention.

Materials and Methods

Tumor Samples and Immunohistochemistry

All tumor samples were collected from the archives of the Institute of Pathology, University of Cologne (Cologne, Germany). The samples were formalin fixed and paraffin embedded (FFPE) as part of routine diagnostic procedures. Clinicopathologic data were obtained from case records provided by the Institute of Pathology, University of Cologne. All tumors were clinically and pathologically identified as being the primary and only neoplastic lesion and classified according to World Health Organization guidelines. Briefly, 3-µm-thick sections of FFPE tumors were deparaffinized, and antigen retrieval was performed by boiling the section in citrate buffer at pH 6 for 20 minutes. Primary antibodies used were given as follows: YAP (1:100, #4912; Cell Signaling Technology, Danvers, MA), endothelin-2 (EDN2; 1:100, NBP1-87942; Novus Biologicals, Littleton, CO), SAV1 (1:100, clone 3B3; Abnova, Taipei, Taiwan), and cytokeratin (1:200, clone AE1/AE3; Dako, Glostrup, Denmark). Staining was performed following established routine procedures, and staining intensity was evaluated individually in a blinded fashion. Statistical analysis was performed using Fisher exact test on GraphPad's QuickCalcs platform (http://graphpad.com/quickcalcs/contingency1.cfm). $P < .05$ was considered statistically significant.

Cell Lines

Human RCC cell lines A498 (ATCC HTB-44), Caki-2 (ATCC HTB-47), MZ1774, B1, B3, and RCC177 were cultured in RPMI 1640 (PAA Laboratories, Pasching, Austria), supplemented with 10% FBS, 1× penicillin/streptomycin (both PAA Laboratories), as well as 5 µg/ml plasmocin (InvivoGen, San Diego, CA). MZ1774, B1, B3, and RCC177 are primary RCC cell lines and have been described in [8-10]. The human RCC cell line ACHN (ATCC CRL-1611) was maintained in Dulbecco's modified Eagle's medium (PAA Laboratories) supplemented with 10% FBS, 1× penicillin/ streptomycin (both PAA Laboratories), and 5 µg/ml plasmocin (InvivoGen).

293FT cells were maintained in Dulbecco's modified Eagle's medium containing 10% FBS, 0.1 mM non-essential amino acids, 1 mM sodium pyruvate, and 1× penicillin/ streptomycin (all PAA Laboratories) as well as 5 µg/ml plasmocin (InvivoGen).

All cell lines were cultured in a humidified atmosphere at 37°C in the presence of 5% CO_2 and were regularly monitored for *Mycoplasma* infection using a polymerase chain reaction (PCR)–based assay as previously described [11].

Lentivirus Production and Generation of Stable Cell Lines

A target set containing shRNA sequences directed against human YAP1 in pLKO.1 lentiviral plasmids was obtained from Thermo Scientific (Waltham, MA), and two clones, which had shown best knockdown efficiency in preliminary experiments, were selected for lentiviral transduction of ccRCC cell lines, designated YAPshRNA#4 (Clone No. TRCN0000107268) and YAPshRNA#5 (Clone No. TRCN0000107269).

293FT-packaging cells were cotransfected with pCMV-VSVg, pCMV-dR8.74, and the respective pLKO.1 plasmids using Fugene6 (Roche Applied Science, Mannheim, Germany). An empty pLKO.1 vector containing no shRNA sequence was used as a negative "mock" control. Supernatant containing lentivirus was harvested after 48 and 72 hours and used to transduce human ccRCC cell lines. Puromycin selection of resistant ccRCC cells was performed, and cells were cultured in the presence of puromycin throughout all experiments.

Cell Viability Assays

Determination of cell viability was performed using the 3-(4,5-dimethyl-2-yl)-5-(3-carboxymethoxyphenyl)-2-(4-sulfophenyl)-2*H*-tetrazolium (MTS) assay as previously described [12]. Briefly, 2000 cells per well were incubated in full growth media for 0, 48, or 96 hours, respectively. All experiments were set up in quadruplicates, and results were normalized to the mean cell viability at 0 hour. CellTiter 96 Aqueous One solution (20 µl; Promega, Madison, WI) was added to each well and absorbance at 492 nm was determined using a 96-well plate reader (BMG Labtech, Offenburg, Germany) on incubation of plates at 37°C for 2 hours.

Replating Efficiency Assays

Cells were seeded into six-well plates at 1000 cells per well in full growth media. Once colonies became visible, cells were fixed with 70% ethanol and stained with a 0.05% aqueous solution of crystal violet (Sigma-Aldrich, Steinheim, Germany). Colonies were counted and colony counts were normalized to the mean colony count of mock-transduced cell lines.

Soft Agar Assays

Soft agar assays were set up in six-well plates with a bottom layer of 1% agarose (Life Technologies, Darmstadt, Germany), an intermediate layer containing 0.6% agarose and 10,000 cells per well, as well as a final layer of media only. Plates were incubated for 4 weeks at 37°C and medium was exchanged once weekly. Colonies were stained with a 0.05% aqueous solution of crystal violet (Sigma-Aldrich) and visualized by trans-UV illumination (Bio-Rad, Hercules, CA). Colonies were counted and colony counts were normalized to the mean colony count of mock-transduced cell lines.

Migration Assays

Modified Boyden chamber assays were set up in 24-well transwell plates with 8-µm pore size filters (BD Biosciences, San Jose, CA). Fifty thousand cells per well were applied and transwell migration was assessed after 48 and 72 hours of incubation at 37°C, respectively. Cells adherent at the bottom of the filter were fixed in 70% ethanol and stained with hematoxylin. Cells were counted in three randomly selected microscopic fields and means and SDs were calculated.

Western Blot

Cells were lysed in radioimmunoprecipitation assay buffer (1% Igepal CA 630, 0.5% Na-deoxycholate, 0.1% sodium dodecyl sulfate, 2 mM EDTA) supplemented with protease and phosphatase inhibitor cocktails (Sigma-Aldrich). Fifty micrograms of total protein was separated on sodium dodecyl sulfate–polyacrylamide gels and transferred onto nitrocellulose membranes (Merck Millipore, Billerica, MA). The blots were probed with antibodies against YAP, phospho-YAP (pYAP), and glyceraldehyde 3-phosphate dehydrogenase (GAPDH) (Cell Signaling Technology) as well as TEAD1 (Santa Cruz Biotechnology, Dallas, TX). Secondary, HRP-coupled antibodies directed against rabbit or mouse IgG, respectively, were purchased from Cell Signaling Technology. Detection was performed as previously described [13].

Transcriptomic Profiling of MZ1774 YAP Knockdown Cells

A total of 100 ng of total RNA, isolated using the RNeasy Kit (Qiagen, Hilden, Germany) following the standard procedure as recommended by the manufacturer, was subjected to a single round of *in vitro* transcription and biotin labeling (Illumina TotalPrep RNA Amplification Kit; Ambion, Austin, TX). The resulting complementary RNA was hybridized on HumanHT-12 v4.0 Expression BeadArrays (Illumina, San Diego, CA) according to the manufacturer's protocols using an automated liquid handling pipeline and scanned on an iScan System.

Expression data were exported as unnormalized sample and control probe profiles from the Illumina GenomeStudio software and analyzed using R/Bioconductor and limma. Data were quality weighed, background-corrected, quantile-normalized, log-transformed, and explored for differentially expressed genes with a false discovery rate (FDR) of 0.05 using Bayesian statistics. Differential regulation of signaling pathways was performed using the signaling pathway impact analysis algorithm as previously described elsewhere [14].

RNA Extraction and Reverse Transcription–Quantitative PCR

For real-time reverse transcription–quantitative PCR (RT-qPCR) analysis, cells were lysed and total RNA was extracted using RNeasy Mini Kit including an on-column DNase digestion step (both Qiagen). RNA was reverse transcribed using random primers and the High Capacity cDNA Reverse Transcription Kit (Life Technologies) according to the manufacturer's specifications. Real-time qPCR for human YAP, endothelin-1 (EDN1), EDN2, V-myc myelocytomatosis viral oncogene homolog (avian) (MYC), cadherin-6 (CDH6), cysteine-rich, angiogenic inducer, 61 (CYR61), thrombospondin-1 (THBS1), and growth arrest and DNA damage-inducible, beta was performed using the SYBR Premix Ex Taq (Tli RNase H Plus) Kit (Takara Bio Europe, Saint-Germain-en-Laye, France) on a Reaplex^2 Mastercycler Real-Time PCR System (Eppendorf, Hamburg, Germany). Relative fold expression levels were determined using the $2(-\Delta\Delta C_t)$ method [15], with GAPDH used as a housekeeping control.

Chromatin Immunoprecipitation

TEAD1-binding sites found in 5 kb upstream of the transcription start site of the indicated genes were considered and primer pairs for qPCR measurement of immunoprecipitated promoter fragments flanking the putative binding regions were designed. Chromatin from formaldehyde cross-linked MZ1774 cells was isolated and sheared to an average fragment size of 600 bp using a probe sonicator (Branson Ultrasonics, Danbury CT). Aliquots of pre-cleared, diluted chromatin was immunoprecipitated using antibodies against YAP or TEAD1 (both Santa Cruz Biotechnology), and immunoprecipitated fragments were pulled down using protein A agarose beads. Immunoprecipitations using normal mouse IgG (Santa Cruz Biotechnology) as well as anti-acetyl histone H3 (Merck Millipore) were carried out simultaneously as negative and positive controls. Immunoprecipitated DNA fragments were purified using the phenol/chloroform method and RT-qPCR for the putative binding regions was performed on all chromatin immunoprecipitation (ChIP) preparations. Fold enrichments were calculated in relation to the negative controls using normal mouse IgG.

Xenograft Experiments

All animal experiments described were approved by the Government of the State of North Rhine-Westphalia (Permit No. 8.87-50.10.37.09.264). Mice were maintained according to the guidelines of the Federation of European Laboratory Animal Science Associations.

To generate subcutaneous xenografts, ACHN YAP knockdown and ACHN mock-transfected cells in log growth phase were harvested by trypsinization, counted, and subsequently injected into the flanks of five male athymic CD1$^{nu/nu}$ mice (Charles River, Wilmington, MA) as previously described [16]. In brief, 2.5×10^6 cells suspended in a total volume of 250 µl [full growth medium/Matrigel (BD Biosciences), 1:1 (vol/vol), prechilled to 4°C] were subcutaneously injected into the flanks of 6- to 8-week-old mice. Starting 10 days after the injection of tumor cells, tumor dimensions were determined twice a week by use of digital calipers (Milomex, Pulloxhill, United Kingdom), and tumor volumes (V) were determined as $V = 1/2(ab^2)$, with a being the longest and b the shortest orthogonal tumor diameter. Mice were sacrificed after 6 weeks, and tumors were harvested and cryopreserved or formalin-fixed for later analysis.

Statistical Analysis

Fisher exact test and two-tailed Student's t-tests were done using GraphPad Prism for Macintosh, version 4.0a. $P < .05$ was regarded to be statistically significant. Unless indicated otherwise, results are shown as means ± SEM.

Results

The Hippo Pathway Effector Yes-Associated Protein Is Overexpressed in ccRCC

In a panel of seven ccRCC cell lines, basal YAP expression was found in all cell lines examined, although expression levels varied greatly, with some cell lines expressing very high levels of YAP, while expression was minimal in others. The phosphorylated form of the transcriptional coactivator constitutes the inactive form of YAP. We found that cell lines with high basal levels of total YAP contained minimal (ACHN) to absent (MZ1774) levels of pYAP pointing toward high transcriptional activity of YAP. We further found consistently high levels of TEAD1, a major interaction partner of YAP, in all cell lines analyzed (Figure 1).

Next, expression of the Hippo pathway component SAV1 and of the nuclear effector of the Hippo pathway YAP was assessed in 31 ccRCC cases by immunohistochemistry. In non-neoplastic renal parenchyma, we observed strong nuclear YAP expression in podocytes and differential expression in the proximal and distal compartments of

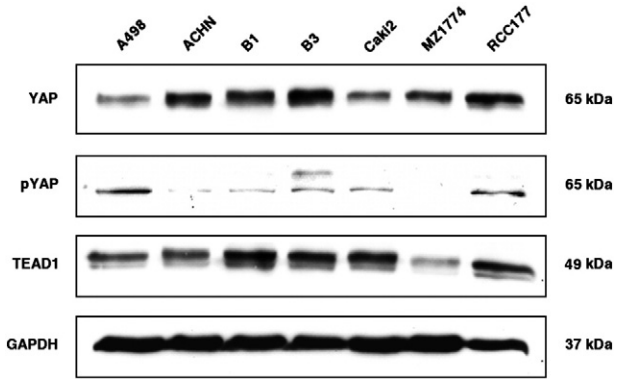

Figure 1. Expression of YAP in ccRCC cell lines. Basal expression of YAP was observed in all ccRCC cell lines examined, whereas expression of the inactive form pYAP was minimal to absent in cell lines expressing high basal levels of YAP. The transcription factor TEAD1, a major interaction partner of YAP, was found in all ccRCC cell lines analyzed.

the renal tubules. While the distal segments of the renal tubule consistently exhibited strong cytoplasmic and nuclear immunolabeling, significantly weaker YAP expression was observed in the proximal tubules, the putative site of origin of ccRCC (Figure 2, *A* and *B*). In RCC tissue samples, we found nuclear up-regulation of YAP expression compared to the proximal tubules in the adjacent normal tissue in 20 of 31 cases (65%; $P < .0001$).

Of note, YAP staining intensity was considerably more prominent at the tumor margins representing the invasive front, and in several patients that showed high expression levels of YAP, we observed single keratin-positive tumor cells invading the surrounding lymphocyte rich stroma, suggesting a possible role of Hippo signaling in ccRCC tumor cell invasion *in vivo* (Figure 2, *C–G*).

We cannot report correlation of YAP positivity with tumor grade based on this small sample size, with 22 of 31 cases being histopathologically classified as grade 2. However, vascular invasion or lymph node metastases were reported for 9 of 30 cases, and of these, 7 exhibited marked YAP positivity.

Table 1. Loss of SAV1 Immunoreactivity Correlates with Nuclear Localization of YAP.

		YAP Expression		
		Cytoplasmic	Nuclear	Total
SAV1	Positive	13	2	15
	Weak or negative	6	10	16
	Total	19	12	31

Fisher exact test, $P = .0091$.

Loss of SAV1 Immunoreactivity Correlates with Nuclear Localization of YAP

Immunohistochemistry revealed strong cytoplasmic SAV1 expression in normal tubular epithelial cells, but curiously immunolabeling was lost in adjacent neoplastic cells in 16 of 31 cases. Moreover, weak or absent SAV1 expression was found to correlate with nuclear localization of YAP, whereas sustained SAV1 expression *vice versa* caused nuclear exclusion of YAP ($P = .0091$; see Table 1 and Figure 2, *H–K*).

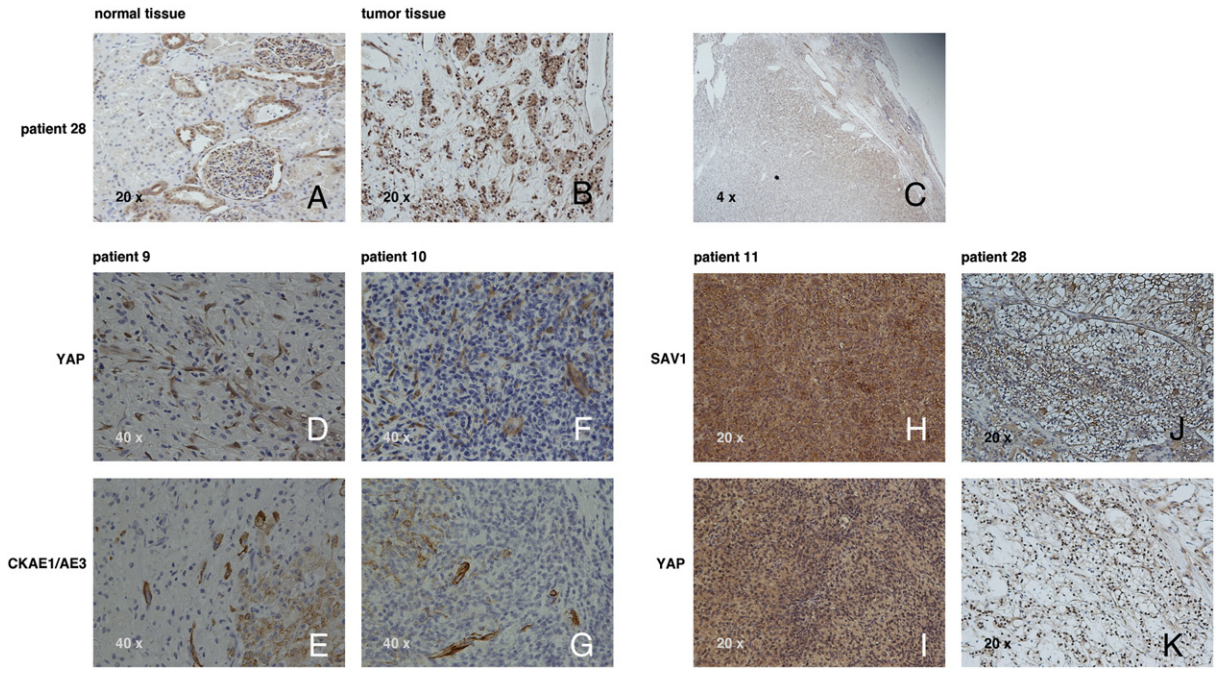

Figure 2. Loss of SAV1 expression results in nuclear sequestration of YAP in patients with ccRCC, and coexpression of YAP and keratin is associated with a highly invasive phenotype. Immunohistochemistry of tumor tissues of 31 patients with ccRCC showed distinct staining of normal renal parenchyma with proximal tubule cells exhibiting only minimal to weak nuclear staining (A), whereas most tumors showed moderate to strong YAP immunoreactivity (B). YAP positivity was stronger at the tumor margins (C) and highlights single cells invading tumor-adjacent stroma (D, F) that also exhibit positivity for cytokeratin (E, G). Loss of SAV1 immunoreactivity was frequently associated with sequestration of YAP expression to the nucleus of tumor cells (J, K), whereas retained SAV1 expression results in mainly cytoplasmic YAP expression (H, I).

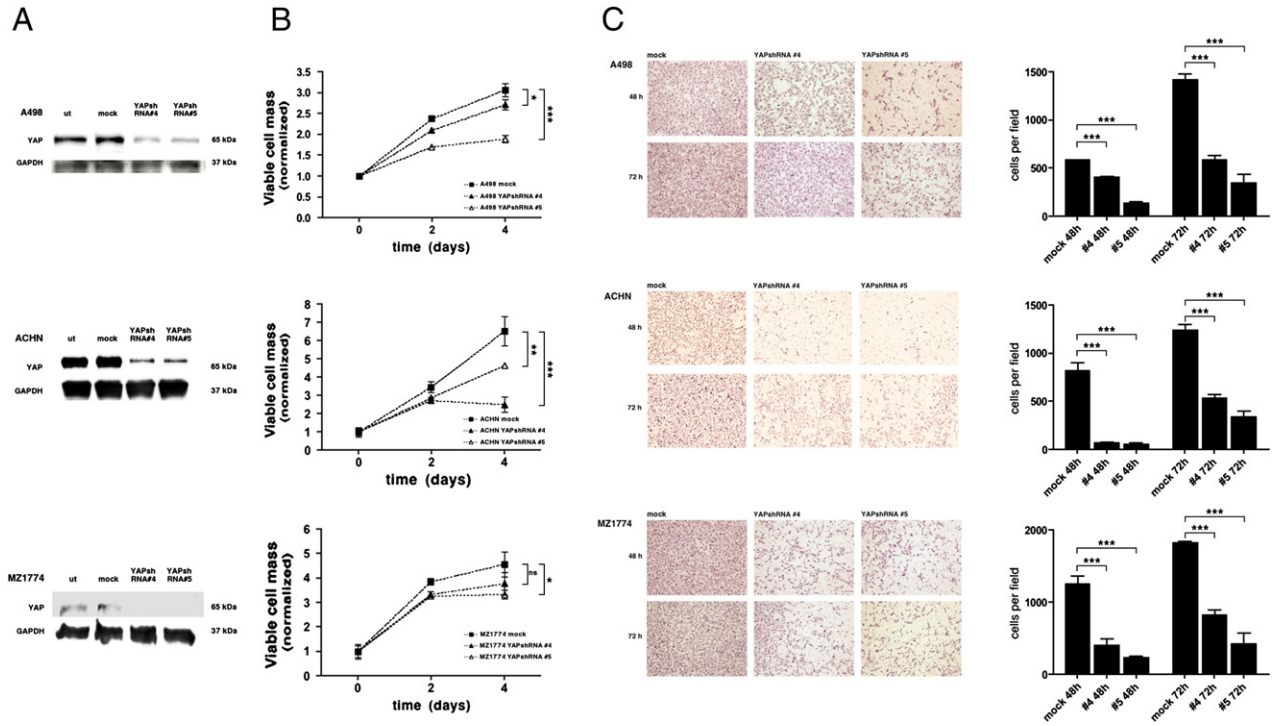

Figure 3. YAP down-regulation impairs proliferation and migration of ccRCC cell lines. shRNA-mediated knockdown of YAP in three different ccRCC cell lines that express high levels of YAP (A) resulted in significantly reduced cell viability as determined by MTS assay (B). YAP down-regulation further resulted in marked inhibition of ccRCC migration in modified Boyden chamber assays. Transwell migration through 8-μm pore filters was assessed after 48 and 72 hours. A pronounced decrease in cell numbers was found for the YAP knockdown mass clones. *P < .05, **P < .01, ***P < .001 (C). Three randomly selected microscopic fields of representative experiments were selected and cells were counted. Results are shown as means ± SD.

shRNA-Mediated Knockdown of YAP Impairs Proliferation and Blocks Migration of ccRCC Cells In Vitro

To further study the role of Hippo signaling in renal cell cancer and to evaluate its potential as a putative therapeutic target, three ccRCC cell lines with high basal YAP expression levels—A498, ACHN, and MZ1774—were picked and dysfunctional Hippo signaling and aberrant YAP activity were abrogated by shRNA-mediated knockdown. For each of the respective parental cell lines, at least two different shRNA sequences directed against YAP (designated as "YAPshRNA#4" and "YAPshRNA#5") were used and compared to untransduced as well as to mock-transduced mass clones to minimize the risk of unspecific, off-target effects. Consistent stable knockdown of endogenous YAP was confirmed by Western blot analysis (Figure 3*A*).

In all of the three cell lines examined, YAP knockdown led to a significant time-dependent reduction of net cell growth compared to mock-transduced cells as determined using MTS assays (Figure 3*B*).

Next, effects of YAP knockdown on *in vitro* cell migration was assessed by employing modified Boyden chamber assays. Of note, a marked reduction of ccRCC migration was observed in response to YAP knockdown in all three cell lines examined (P < .001; Figure 3*C*), in line with the observation of YAP being associated to an invasive phenotype *in vivo*, as already discussed above. All experiments were done in triplicates and repeated at least once.

YAP Knockdown Diminishes Colony Formation and Anchorage-Independent Growth of ccRCC Cells

The ability to form colonies from single cells and the ability to grow anchorage independently are considered two important hallmarks of cancer cells *in vitro*. To determine potential effects of YAP knockdown on the former of these cellular functions in ccRCC, replating efficiency assays were performed using single cell suspensions. Of note, the ability of ACHN-YAP-shRNA#4 cells to form colonies from single cells in this setting was significantly reduced compared to mock-transduced ACHN controls (mean reduction of colony counts by 66.3 ± 0.05%, n = 6, P < .0001; Figure 4*A*). Of interest, the colonies formed by YAP knockdown cells were not only less numerous but also smaller in size, reflecting reduced *in vitro* net cell growth as already observed previously in MTS assays.

Anchorage-independent growth and colony formation in soft agar is a widely accepted *in vitro* surrogate phenotype for malignant transformation. YAP knockdown potently and reproducibly abrogated anchorage-independent growth of ACHN cells in soft agar (reduction of colony counts by more than 90 ± 0.02%, n = 6, P < .0001; Figure 4*B*). Similar to what was seen in replating assays, the remaining colonies formed by ACHN-YAP-shRNA mass clones were not only sparse in number but also significantly smaller compared to their mock-transduced counterparts in this three-dimensional culture setting.

YAP Knockdown Inhibits Tumor Growth in a Subcutaneous Xenograft Model of ccRCC

On the basis of these encouraging *in vitro* data suggesting a dependency of ccRCC cells on signaling through the Hippo pathway for maintenance of a malignant phenotype, we next tried to assess the *in vivo* relevance of this finding using a subcutaneous xenograft model. Male athymic CD1$^{nu/nu}$ nude mice, 6 to 8 weeks of age, were injected subcutaneously with 2.5 × 10^6 ACHN-YAP-shRNA or ACHN mock cells into both flanks. Tumor volumes were assessed

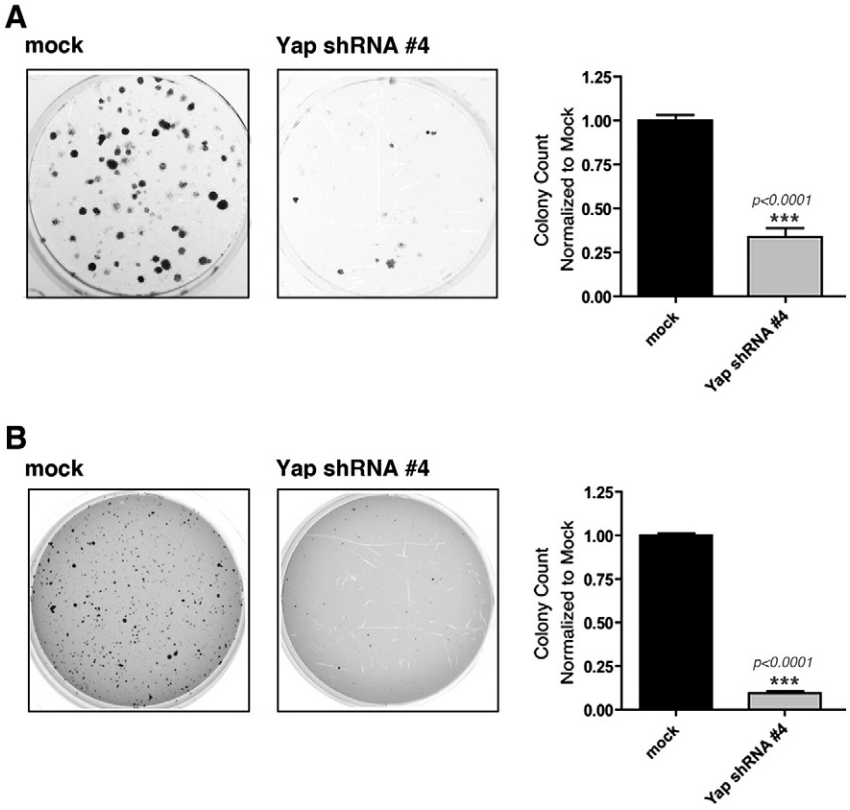

Figure 4. shRNA-mediated YAP knockdown reduces colony formation and abates anchorage-independent growth of ccRCC cells. Downregulation of YAP significantly reduced the number of colonies formed in replating efficiency assays (A) as well as anchorage-independent growth in soft agar of the ccRCC cell line ACHN (B). Representative images and combined colony counts of three independent experiments are shown.

weekly using digital calipers starting 1 week after injection. Of note, xenograft growth of ACHN-YAP-shRNA cells was significantly delayed compared to ACHN mock controls ($P = .0182$; Figure 6, *A*, *left panel*, and *B*), while at the same time the overall body mass of xenograft-bearing mice was not significantly altered between the two study arms (Figure 6*A*, *right panel*).

At 5 weeks after injection, mice were sacrificed, and tumors were harvested for histopathologic and immunohistochemical evaluation or snap-frozen for mRNA extraction and subsequent real-time RT-qPCR analysis, respectively.

Microarray Analysis of MZ1774 YAP Knockdown Cells Identifies Putative Downstream Targets of YAP in ccRCC

cDNA microarray analysis of MZ1774 YAPshRNA mass clones revealed 14 genes that were upregulated more than two-fold (Table 2) and another 42 genes that were downregulated by more than 50%

Table 2. Upregulated Genes in MZ1774 YAP Knockdown Cells.

Gene ID	Symbol	Gene Name	Accession No.	Fold Change	*P* Value
84952	*CGNL1*	*Cingulin-like 1*	NM_001252335.1	2.97	2.23E−11
5265	*SERPINA1*	*Serpin peptidase inhibitor, clade A (alpha-1 antiproteinase, antitrypsin), member 1*	NM_000295.4	2.49	6.10E−07
80117	*ARL14*	*ADP-ribosylation factor-like 14*	NM_025047.2	2.49	1.91E−07
10344	*CCL26*	*Chemokine (C-C motif) ligand 26*	NM_006072.4	2.47	2.00E−05
1004	*CDH6*	*Cadherin-6, type 2, K-cadherin (fetal kidney)*	NM_004932.3	2.27	7.61E−10
266977	*GPR110*	*G protein–coupled receptor 110*	NM_153840.2	2.22	5.90E−07
283460	*HNF1A-AS1*	*HNF1A antisense RNA 1 (non-protein coding)*	NR_024345.1	2.11	2.20E−04
55195	*C14orf105*	*Chromosome 14 open reading frame 105*	NM_018168.2	2.07	4.97E−03
266977	*GPR110*	*G protein–coupled receptor 110*	NM_153840.2	2.06	1.09E−06
11074	*TRIM31*	*Tripartite motif containing 31*	NM_007028.3	2.04	1.00E−05
55775	*TDP1*	*Tyrosyl DNA phosphodiesterase 1*	NM_001008744.1	2.03	7.20E−04
283209	*PGM2L1*	*Phosphoglucomutase 2-like 1*	NM_173582.3	2.02	5.00E−05
5265	*SERPINA1*	*Serpin peptidase inhibitor, clade A (alpha-1 antiproteinase, antitrypsin), member 1*	NM_000295.4	2.02	1.30E−04
11221	*DUSP10*	*Dual specificity phosphatase 10*	NM_007207.4	2.01	1.00E−04
3767	*KCNJ11*	*Potassium inwardly rectifying channel, subfamily J, member 16*	NM_000525.3	1.97	1.00E−05
2353	*FOS*	*FBJ murine osteosarcoma viral oncogene homolog B*	NM_005252.3	1.97	5.91E−02
56829	*ZC3HAV1*	*Zinc finger CCCH-type, antiviral 1*	NM_020119.3	1.97	1.50E−04
158295	*MGC24103*	*Hypothetical MGC24103*	XR_108934.3	1.96	4.91E−03
7327	*UBE2G2*	*Ubiquitin-conjugating enzyme E2G2*	NM_003343.5	1.95	8.77E−03
56664	*VTRNA1-1*	*Vault RNA 1-1*	NR_026703.1	1.94	1.20E−04

compared to mock-transfected MZ1774 cells (Table 3). Of these, eight targets were picked for validation by real-time qPCR. All of those eight targets found to be downregulated by microarray analysis were confirmed to be downregulated using RT-qPCR, and CDH6 as an example of a target found to be overexpressed in the microarray analysis was also found to be upregulated using RT-qPCR (Figure 5*A*).

Increasing recent evidence suggests that the complexity of cancer genomic and transcriptomic patterns might only be fully appreciated in its entirety when moving away from analyzing abnormalities on a single-gene basis and toward a pathway-based approach. This fundamental paradigm shift is currently being more and more commonly adapted and is finding its way into basic understanding of cancer research as well as into everyday routine clinical applications in the field of medical oncology [17,18]. To identify signaling pathways potentially affected by altered signaling through the Hippo/warts axis, signaling pathway impact analysis was performed as previously described elsewhere [14]. Of note, the top three pathways found to be affected were the p53, MAP kinase, as well as cell cycle progression pathways, all of which have long been well established as centrally involved in carcinogenesis and maintenance of a malignant phenotype across several tumor entities (Table 4). These findings thus further support our hypothesis that Hippo signaling might be a crucial driver of carcinogenesis and represents a promising potential therapeutic target in ccRCC.

Among the most prominently downregulated genes were two members of the endothelin family, *EDN1* and *EDN2*, as well as *c-Myc*. Cross-validation of mRNA expression of these genes in MZ1774, A498, and ACHN YAP knockdown cells confirmed significant *c-Myc* and *EDN1* down-regulation in MZ1774 and A498 on YAP knockdown (MZ1774: fold changes = 0.34 ± 0.006, $P < .0001$ for *c-Myc* and 0.41 ± 0.009, $P < .0001$ for *EDN1*; A498: fold changes = 0.79 ± 0.026, $P = .0085$ for *c-Myc* and 0.41 ± 0.019, $P = .0001$ for *EDN1*, respectively; see Figure 5*B*). *EDN2* expression was significantly reduced in all three cell lines examined (fold changes = 0.06 ± 0.003, $P < .0001$ for MZ1774, 0.62 ± 0.025, $P = .001$ for A498, and 0.17 ± 0.0067, $P < .0001$ for ACHN, respectively).

Of note, immunohistochemistry and real-time RT-qPCR confirmed consistent knockdown of YAP1 as well as down-regulation of

Table 3. Downregulated Genes in MZ1774 YAP Knockdown Cells.

Gene ID	Symbol	Gene Name	Accession No.	Fold Change	*P* Value
1907	*EDN2*	*Endothelin-2*	NM_001956.3	0.24	1.16E–11
1906	*EDN1*	*Endothelin-1*	NM_001955.4	0.31	8.57E–06
7057	*THBS1*	*Thrombospondin-1*	NM_003246.2	0.33	2.34E–05
4616	*GADD45B*	*Growth arrest and DNA-damage-inducible, beta*	NM_015675.3	0.34	7.53E–05
3491	*CYR61*	*Cysteine-rich, angiogenic inducer, 61*	NM_001554.4	0.36	1.73E–04
10175	*CNIH*	*Cornichon homolog (Drosophila)*	NM_005776.2	0.37	3.02E–06
1646	*AKR1C2*	*Aldo-keto reductase family 1, member C2 (dihydrodiol dehydrogenase 2; bile acid binding protein; 3-alpha hydroxysteroid dehydrogenase, type III)*	NM_001354.5	0.37	4.71E–06
4609	*MYC*	*V-myc myelocytomatosis viral oncogene homolog (avian)*	NM_002467.4	0.37	1.05E–06
523	*ATP6V1A*	*ATPase, H^+ transporting, lysosomal 70 kDa, V1 subunit A*	NM_001690.3	0.38	4.44E–12
4609	*MYC*	*V-myc myelocytomatosis viral oncogene homolog (avian)*	NM_002467.4	0.38	2.34E–06
6520	*SLC3A2*	*Solute carrier family 3 (activators of dibasic and neutral amino acid transport), member 2*	NM_001012662.2	0.39	3.40E–06
284018	*C17orf58*	*Chromosome 17 open reading frame 58*	NM_181655.2	0.39	7.44E–10
10413	*YAP1*	*Yes-associated protein 1*	NM_001130145.2	0.40	2.42E–08
81788	*NUAK2*	*NUAK family, SNF1-like kinase, 2*	NM_030952.1	0.40	4.10E–05
1316	*KLF6*	*Kruppel-like factor 6*	NM_001160124.1	0.40	4.23E–04
586	*BCAT1*	*Branched chain amino acid transaminase 1, cytosolic*	NM_001178091.1	0.41	7.35E–08
81788	*NUAK2*	*NUAK family, SNF1-like kinase, 2*	NM_030952.1	0.41	5.60E–06
6526	*SLC5A3*	*Solute carrier family 5 (sodium/myo-inositol cotransporter), member 3*	NM_006933.4	0.41	1.85E–07
59345	*GNB4*	*Guanine nucleotide binding protein (G protein), beta polypeptide 4*	NM_021629.3	0.42	2.34E–08
54206	*ERRFI1*	*ERBB receptor feedback inhibitor 1*	NM_018948.3	0.42	4.98E–09
27032	*ATP2C1*	*ATPase, Ca^{++} transporting, type 2C, member 1*	NM_001199180.1	0.42	2.63E–07
84706	*GPT2*	*Glutamic pyruvate transaminase (alanine aminotransferase) 2*	NM_001142466.1	0.44	4.04E–08
9518	*GDF15*	*Growth differentiation factor 15*	NM_004864.2	0.44	8.31E–05
406991	*MIR21*	*MicroRNA 21*	NR_029493.1	0.44	4.12E–07
59272	*ACE2*	*Angiotensin I converting enzyme (peptidyl-dipeptidase A) 2*	NM_021804.2	0.44	2.76E–07
8140	*SLC7A5*	*Solute carrier family 7 (amino acid transporter light chain, L system), member 5*	NM_003486.5	0.44	9.39E–07
51125	*GOLGA7*	*Golgin A7*	NM_001002296.1	0.44	1.41E–11
4703	*NEB*	*Nebulin*	NM_001164507.1	0.44	2.93E–05
79660	*PPP1R3B*	*Protein phosphatase 1, regulatory (inhibitor) subunit 3B*	NM_001201329.1	0.44	4.58E–06
10175	*CNIH*	*Cornichon homolog (Drosophila)*	NM_005776.2	0.45	2.71E–05
57761	*TRIB3*	*Tribbles homolog 3 (Drosophila)*	NM_021158.3	0.46	8.68E–06
388272	*C16orf87*	*Chromosome 16 open reading frame 87*	NM_001001436.2	0.46	1.76E–06
6185	*RPN2*	*Ribophorin II*	NM_002951.3	0.46	1.28E–07
27063	*ANKRD1*	*Ankyrin repeat domain 1 (cardiac muscle)*	NM_014391.2	0.47	2.80E–06
29968	*PSAT1*	*Phosphoserine aminotransferase 1*	NM_021154.3	0.47	1.45E–04
2152	*F3*	*Coagulation factor III (thromboplastin, tissue factor)*	NM_001993.4	0.47	4.45E–06
81539	*SLC38A1*	*Solute carrier family 38, member 1*	NM_001077484.1	0.48	1.17E–04
6397	*SEC14L1*	*SEC14-like 1 (S. cerevisiae)*	NM_001039573.2	0.48	3.67E–08
10397	*NDRG1*	*N-myc downstream regulated 1*	NM_001135242.1	0.48	5.34E–06
5638	*PRRG1*	*Proline rich Gla (G-carboxyglutamic acid) 1*	NM_000950.2	0.48	5.42E–08
10797	*MTHFD2*	*methylenetetrahydrofolate dehydrogenase ($NADP^+$ dependent) 2, methenyltetrahydrofolate cyclohydrolase*	NM_006636.3	0.49	7.56E–08
2530	*FUT8*	*Fucosyltransferase 8 (alpha (1,6) fucosyltransferase)*	NM_178155.2	0.49	3.76E–07
80115	*BAIAP2L2*	*BAI1-associated protein 2-like 2*	NM_025045.4	0.49	1.06E–05
5209	*PFKFB3*	*6-Phosphofructo-2-kinase/fructose-2,6-biphosphatase 3*	NM_004566.3	0.49	3.49E–05
10175	*CNIH*	*Cornichon homolog (Drosophila)*	NM_005776.2	0.50	2.86E–05

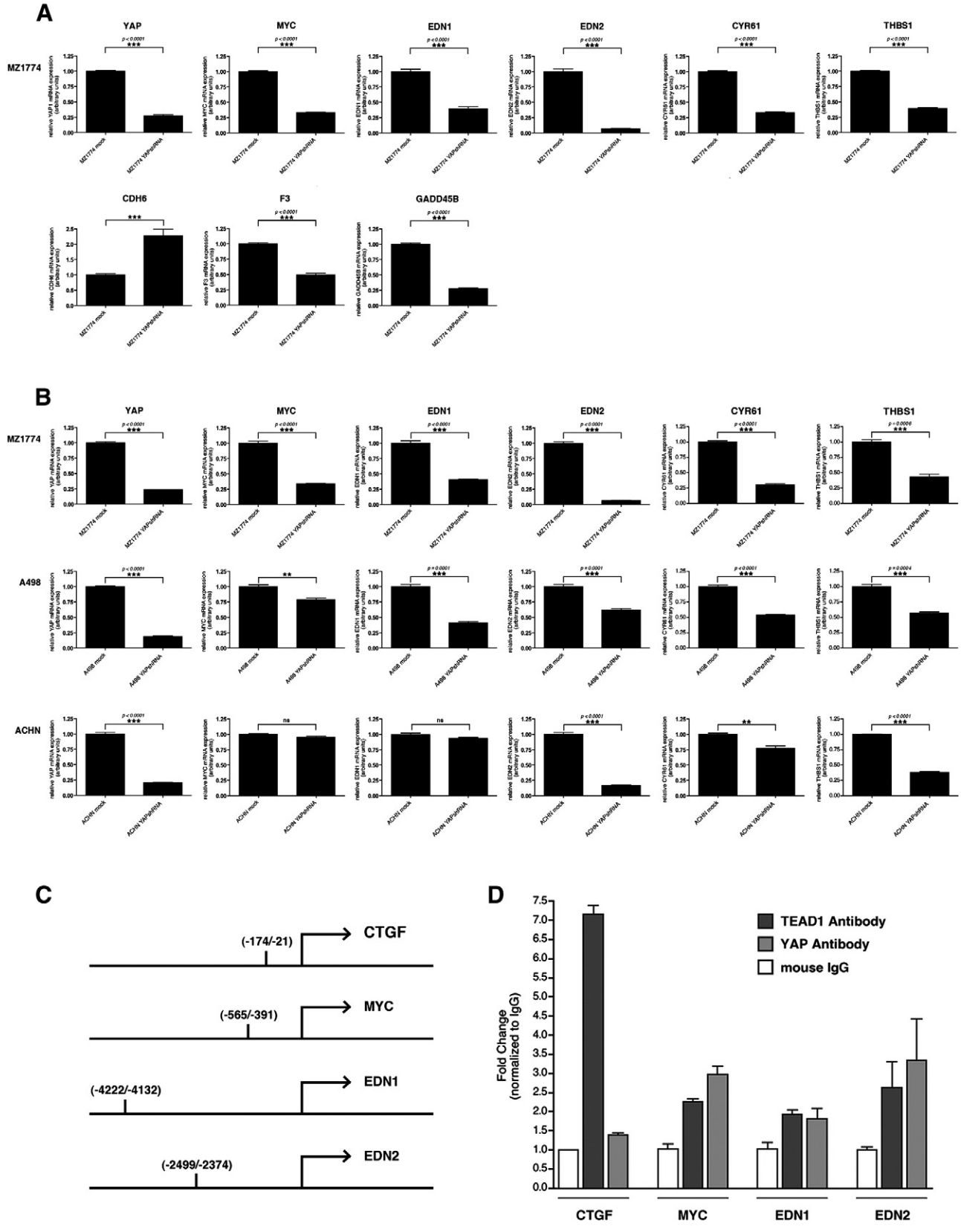

Figure 5. Differential expression of selected genes was confirmed by real-time RT-qPCR. The graphs show normalized average steady-state mRNA expression levels in YAPshRNA-transfected *versus* mock-transfected MZ1774 cells as means and SEM (A). Cross-validation in other YAPshRNA-transfected ccRCC cell lines revealed uniform EDN2, CYR61, and THBS1 down-regulation as well as EDN1 and cMYC down-regulation in two tested cell lines (B). YAP and TEAD1 are simultaneously present on selected TEAD1-binding sites in the promoter regions of CTGF, MYC, EDN1, and EDN2 (C, D).

Table 4. Signaling Pathways Affected by Knockdown of YAP in MZ1774 Cells.

KEGG Pathway	ID	pNDE	pPERT	pG	pGFDR	pGFWER	Status	KEGG Link
p53 signaling pathway	4115	1.524E−06	0.1260	3.1620E−06	0.0003	0.0003	Activated	http://www.genome.jp/dbget-bin/show_pathway?hsa04115+3486+1647+4616+7057+8795+54205+1021+27244
MAPK signaling pathway	4010	1.829E−04	0.3150	6.2009E−04	0.0248	0.0670	Inhibited	http://www.genome.jp/dbget-bin/show_pathway?hsa04010+11221+2247+627+9261+1649+51776+1647+4616+3554+4609+2872
Cell cycle	4110	6.475E−02	0.0010	6.8925E−04	0.0248	0.0744	Activated	http://www.genome.jp/dbget-bin/show_pathway?hsa04110+1647+4616+1021+4609

KEGG, Kyoto encyclopedia of genes and genomes; pNDE, probability value for overrepresentation of differentially expressed genes in a given pathway; pPERT, probability value for abnormal perturbation of that pathway, as measured by propagating measured expression changes across the pathway topology; pG, global probability value combining pNDE and pPERT; pGFDR, pG (after false discovery rate-correction); pGFWER, pG (after familywise error rate-correction).

EDN2, both at the mRNA and protein levels, respectively, in murine xenografts of human ccRCCs as well (Figure 6, *C* and *D*).

To investigate a direct relationship between YAP and its putative target genes in ccRCC, we performed ChIP-qPCR on selected regions containing TEAD-binding motifs within the promoter region of those genes (Figure 5*C*). A well-characterized YAP/TEAD1-binding site in the promoter region of the *bona fide* YAP target gene *CTGF* was selected as a positive control. We found YAP and TEAD to be simultaneously present on the promoter regions of the *MYC*, *EDN1*, as well as *EDN2* genes in MZ1774 (Figure 5*D*).

YAP Expression Correlates with EDN2 Expression in ccRCC Tumors

We next analyzed the expression of the thus identified proposed downstream effector of YAP, EDN2, in primary tissue samples of human ccRCC tumors using immunohistochemistry. YAP expression

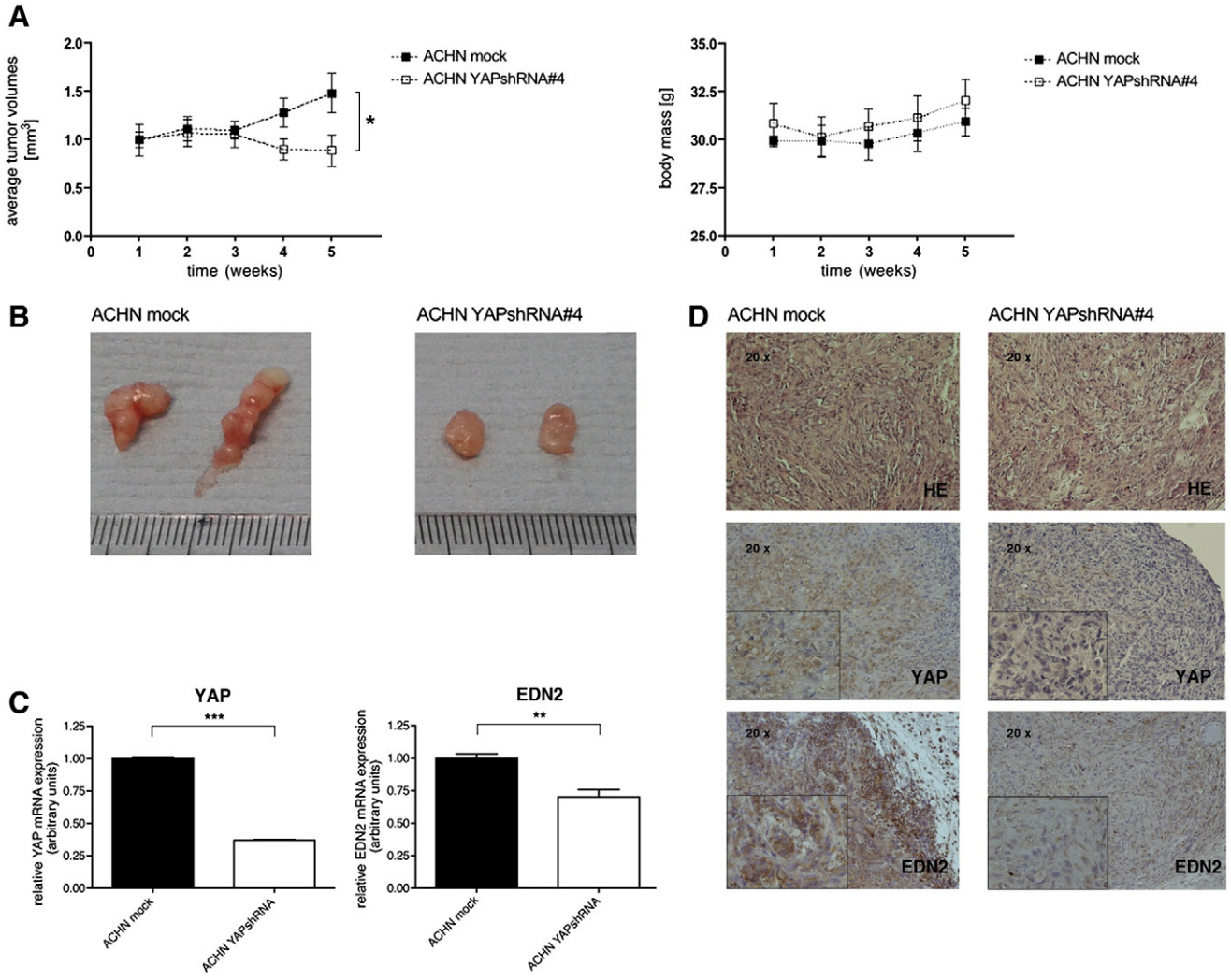

Figure 6. YAP down-regulation inhibits tumor growth in a subcutaneous xenograft model. Subcutaneous injection of YAP knockdown cells into the flanks of CD1$^{nu/nu}$ mice resulted in significantly smaller tumors compared to mock-transduced cells while not affecting the body mass of the mice (A, B). RT-PCR of freshly frozen xenograft tissue confirmed significant down-regulation of YAP and EDN2 in tumors derived from ACHN YAP knockdown cells (C). Hematoxylin and eosin stainings and immunohistochemistry of YAP and EDN2 in ACHN mock and ACHN YAP knockdown xenograft tissues illustrate down-regulation on the protein level (D). Representative images are shown in $\times 20$, with insets in $\times 40$ magnification.

Table 5. Correlation of YAP and EDN2 Expression in ccRCC Tumors.

		YAP Expression		
		Positive	Weak or Negative	Total
EDN2	Positive	20	3	23
	Weak or negative	2	5	7
	Total	22	8	30

Fisher exact test, $P = .0067$.

was found to significantly correlate with positivity for EDN2 ($P = .0067$; Table 5). Figure 7 shows representative examples of two cases exhibiting double positivity (*A* and *B*) or double negativity (*C* and *D*) for YAP and EDN2, respectively.

Finally, Figure 8 summarizes our results and proposes a potential mechanism of the proproliferative and proinvasive functions of YAP in ccRCC by its interaction with the endothelin axis and the tumor microenvironment.

Discussion

Our data presented here suggest widespread deregulation of the Hippo signaling pathway in human ccRCC. In a considerable subset of cases, this was found to be due to down-regulation of the upstream regulator SAV1 and consecutive nuclear accumulation of YAP. In this regard, our data are in line with a recent report by Matsuura and colleagues, who describe down-regulation of SAV1 in high-grade ccRCC [19]. Of note, copy number loss on chromosome 14q22, i.e., in the region of the *SAV1* gene, have been previously described in high-grade ccRCC by different groups [19-21]. In addition, truncating mutations of this upstream member of the Hippo network are present in a subset of VHL-wt ccRCCs [22,23]. However, our data presented here also hint at the existence of other alternative mechanisms of pathway perturbation in human ccRCC, since in a considerable subset of cases in which marked, albeit not exclusively nuclear staining for YAP was observed this was not accompanied by loss of SAV1 expression.

Moreover, our data suggest an important role of Hippo signaling in mediating proliferation as well as migration and invasion, both *in vitro* and *in vivo*, with obvious impact on the metastatic potential of ccRCC. In line with our observations, conditional knockout of NF2, an upstream activator of the growth inhibitory Hippo pathway, in the proximal tubular epithelium of Villin-Cre;$Nf2^{(lox/lox)}$ mice leads to intratubular neoplasia and invasive carcinoma that resembles human RCC in a mouse model of RCC [24]. Recent reports also linked the renal cilia-associated proteins NPHP4 and NPHP9 to Hippo signaling in both oncogenically transformed and normal kidney epithelial cells. These proteins were found to prevent Lats-dependent phosphorylation of YAP, thus controlling YAP activation and mediating cell proliferation [25,26]. Of note, Lamar et al. recently described enhanced metastatic potential of breast cancer as well as melanoma cells with increased YAP/TEAD activity; they concluded that YAP can promote metastasis through its TEAD-interaction domain [27]. To the best of our knowledge, our data presented here for the first time hint at a possible link between Hippo signaling and increased invasiveness and metastatic potential in ccRCC.

As a next step, we thought to further dissect the underlying mechanism by which YAP exerts its proproliferative and potentially proinvasive properties in ccRCC on a molecular level and to identify downstream effectors of Hippo signaling in this entity, since this might have important implications in exploiting this pathway as potential therapeutic target in future work. Transcriptomic profiling of MZ1774 YAP knockdown cells provided clues toward downstream targets of YAP in ccRCC, including some genes that are known to be overexpressed in ccRCC like members of the endothelin family, c-Myc, and CDH6, and has been shown to promote tumor growth and metastasis in experimental settings. We observed consistent down-regulation of the *bona fide* YAP target gene *CYR61* on YAP knockdown in all cell lines examined. CYR61 is a positive regulator of cell growth [28] and has been implicated as a proangiogenic factor in highly vascularized RCC, acting alongside vascular endothelial growth factor (VEGF) and exerting additive nonoverlapping

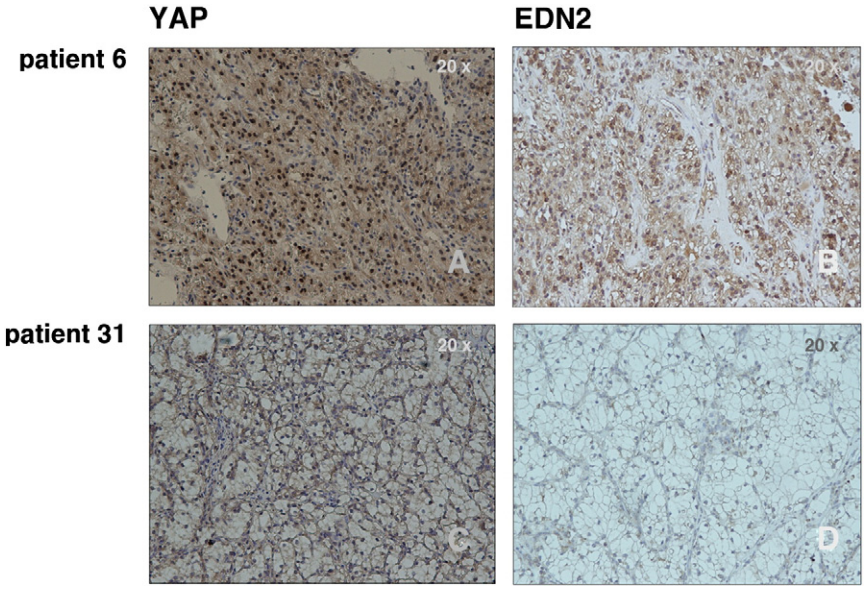

Figure 7. EDN2 expression correlates with YAP positivity in patients with ccRCC. Immunohistochemistry of tumor tissues of 30 patients with ccRCC confirmed that EDN2 expression correlates with YAP positivity. Double positivity for YAP and EDN2 was frequently observed (A, B), whereas loss of YAP expression often results in minimal to absent EDN2 expression (C, D).

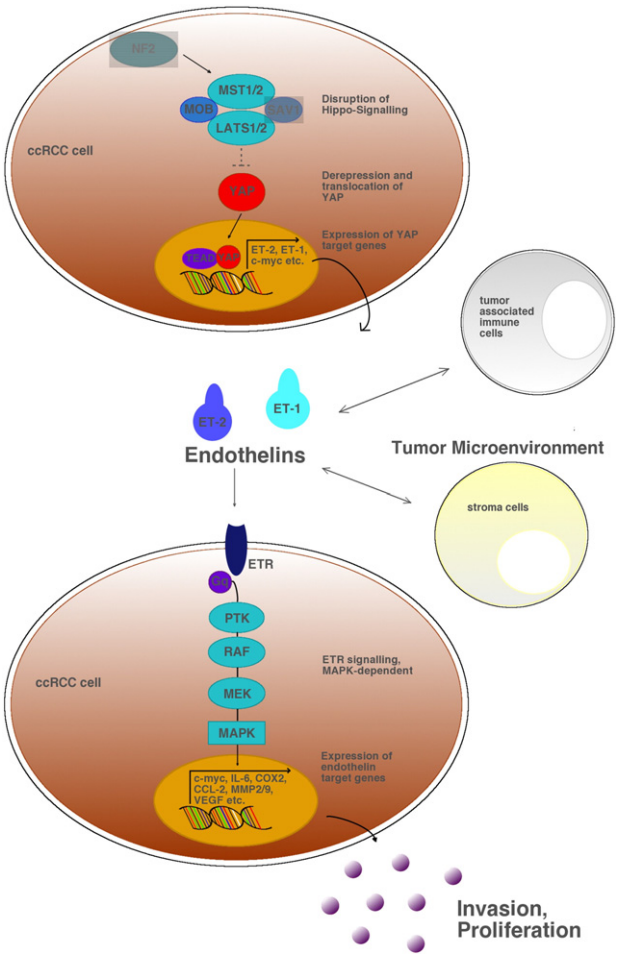

Figure 8. Putative interaction of YAP with the endothelin axis in ccRCC.

functions [29]. CYR61 up-regulation correlated with loss of von Hippel-Lindau protein expression, although its expression was only partly dependent on Hypoxia-inducible factor 2-alpha function, suggesting additional mechanisms that contribute to CYR61 up-regulation in RCC [29]. Furthermore, recent reports linked CYR61 with integrin-mediated cell migration and invasion in prostate cancer cell lines, hinting at a potential role in metastasis [30].

THBS1 is one of the most potent physiological antiangiogenic factors and its expression has been reported as an independent prognostic factor in ccRCC with retained expression being associated with increased survival [31]. It is therefore somewhat surprising to observe down-regulation of THBS1 mRNA on YAP knockdown in all cell lines analyzed. YAP might interfere with the network of proangiogenic and antiangiogenic factors, such as CYR61 and THBS1, in ccRCC, tipping the balance toward a homeostasis that favors the proliferation and survival of the tumor cells.

EDN1 and *EDN2* were the most prominently downregulated genes in MZ1774 cells on YAP knockdown. Endothelins are important regulators of kidney function, and endogenous endothelin is involved in the regulation of renal cell growth and proliferation, as well as fluid and electrolyte excretion. Production of endothelins in the kidney is increased in numerous renal diseases [32], and ccRCC tumors have been reported to express EDN1 and its receptor ET_A with ccRCC cell lines secreting EDN1 [33,34]. The selective endothelin-A receptor antagonist atrasentan has been used in combination with interferon-alpha in a phase I study in metastatic RCC, albeit with moderate clinical antitumor effects [35].

The impact of YAP knockdown on EDN2 expression was most pronounced and present in all three cell lines tested, whereas EDN1 down-regulation could be cross-validated in A498 but not in ACHN YAP knockdown cells. As ACHN YAP knockdown cells displayed the same phenotype in respect to reduced cancer cell proliferation and migration and did form smaller xenograft tumors *in vivo*, EDN2 seems to be one of the main effectors responsible for these effects. In line with this hypothesis, we found that YAP and EDN2 expression correlates in clinical tumor specimen of patients with ccRCC as assessed by immunohistochemistry. Research on the endothelin axis in cancer has focused mainly on EDN1, and results have largely been extrapolated to EDN2. It has been assumed that EDN2 would mimic the actions of its more abundant counterpart EDN1, but recent findings *in vitro* and in knockout mice underscore that EDN2 does not simply amplify or duplicate EDN1 action and imply a distinct function of EDN2 in physiological and pathophysiological processes [36]. Furthermore, EDN2, and not the more abundant EDN1, was first isolated from RCC cell lines [37]. A recent paper reported EDN2 expression to be a common and early event in patients with localized ccRCC undergoing nephrectomy and proposed a potential role in ccRCC progression [38]. An association of higher tumor expression of EDN2 with longer progression-free survival could not be confirmed after adjustment for known clinicopathologic factors and it would be interesting to compare expression levels with tumors of patients with advanced metastatic disease.

Grimshaw et al. reported an important influence of EDN2 on the invasive potential of breast cancer cells and proposed a mechanism where EDN2-secreting tumor cells provide chemotactic cues to tumor-infiltrating macrophages, which in turn secrete matrix metallopeptidase (MMP)-2 and MMP-9 to facilitate tumor cell invasion and metastasis [39]. The observed effect was dependent on both endothelin receptor B and MAPK signaling, and expression of EDN2 and its receptor was stronger at the invasive margin of the tumor tissue. Of note, we observed inhibition of the MAPK signaling pathway on YAP knockdown in MZ1774 cells. Overexpression of EDN2 increases the invasive potential of breast cancer cell lines *in vitro* but is not sufficient to induce an invasive phenotype in benign cells, indicating the cooperation with other signaling networks [40].

Concurrently, Said et al. reported an instrumental role of EDN1 signaling through endothelin receptor A in the development of metastatic bladder cancer and delineated a proinvasive network governed by members of the endothelin family involving direct actions like the activation of proinflammatory transcription factors such as activator protein 1 and nuclear factor kappa-light-chain-enhancer of activated B cells in human monocytes and cancer cells and the stimulation of the production of a range of proinvasive cytokines like interleukin-6, cyclooxygenase 2, chemokine (C-C motif) ligand 2 (CCL2), MMP-2, and MMP-9 as well as indirect modulation of the tumor microenvironment by influencing tumor-stroma interactions as well as tumor-associated immune cells [41]. These endothelin functions were instrumental in the process of metastatic colonization, the first step of the establishment of a filial tumor at a distant site, and pharmacologic blockade of endothelin receptor signaling inhibited metastasis significantly in an experimental animal model, despite having only modest effects on primary tumor growth. We observed that these reported target genes of EDN1 signaling, namely *interleukin-6*, *COX2*, *VEGFA*, and *CCL2*, were

also moderately but significantly downregulated in MZ1774 YAP knockdown cells as determined by microarray or RT-PCR analysis (fold changes were 0.74, $P < .0008$ for interleukin-6, 0.60, $P = .002$ for COX2, 0.67, $P = .0065$ for VEGFA, and 0.82, $P = .032$ for CCL2, respectively).

Up-regulation of c-Myc expression has been reported to occur in a majority of ccRCC cases [42,43], although amplification of the *MYC* gene is only found in a small subset of cases [42,44] leading to the assumption that c-Myc is activated by other mechanisms in addition to amplification. We observed strong c-Myc down-regulation on YAP knockdown in MZ1774 cells. c-Myc knockdown by siRNA in ccRCC cell lines leads to a phenotype that resembles that of YAP knockdown with marked inhibition of proliferation and anchorage-independent growth [42]. c-Myc expression is stimulated by EDN1 through MAPK signaling in neoplastic cells [45,46], and our data show inhibition of the MAPK signaling pathway along with EDN1 and concomitant c-Myc down-regulation on YAP knockdown in MZ1774 and A498 cells, whereas mRNA expression levels of these genes were not affected in ACHN cells, indicating that c-Myc might additionally be an indirect target of YAP, downstream of EDN1 in ccRCC. However, the *MYC*-promoter region features GT-IIC consensus sequences as potential binding sites for the YAP/TEAD complex, and indeed, these regions are enriched in ChIPs of MZ1774 lysates, underscoring the primary direct relationship. Previous studies have also found pronounced c-Myc up-regulation on overexpression of YAP in the murine liver [3].

CDH6 mRNA expression was found to be upregulated in MZ1774 YAP knockdown cells. Normal renal epithelium and RCC express multiple members of the cadherin family in a distinct pattern with E-cadherin being expressed in Bowman's capsule and all tubular segments except the proximal convoluted and straight tubules [47]. Consequently, E-cadherin expression frequency in RCC is lower than in other cancers and even low-grade tumors infrequently express E-cadherin [48]. Conversely, CDH6 is expressed in proximal renal tubules and RCC, especially when E-cadherin is absent, and seems partly to take over E-cadherin function [49]. Detectable CDH6 mRNA from circulating tumor cells in the peripheral blood of patients with RCC has been proposed as a prognostic marker associated with increased risk of metastasis [49,50] hinting not necessarily at an active role of the CDH6 protein in metastasis but rather highlighting the inadequate ability of CDH6 to replace E-cadherin in cell adhesion. Up-regulation of the cell adhesion molecule CDH6 in response to YAP knockdown is therefore not contradictory to a less invasive phenotype.

In light of the most recent report published by the Cancer Genome Research Atlas Network [51], which found frequently altered promoter methylation of miR-21 with subsequent high miR-21 expression in high stage ccRCCs that inversely correlated with outcome, it is intriguing to note the significant down-regulation of miR-21 upon YAP knockdown. Recent work from Dey et al. showed that miR-21 targets PTEN protein expression and promotes ccRCC survival and invasion through Akt/TORC1 signaling [52].

Taken together, our data provide strong evidence that Hippo signaling plays an important role in regulating proliferation, invasiveness, and metastatic potential of ccRCC and might serve as a target for therapeutic intervention in the future. Disrupted Hippo signaling and consecutive derepression and activation of YAP lead to increased production of the putative YAP target genes *EDN1*, *EDN2*, and *c-Myc*. Increased endothelin signaling in turn results in increased production of proproliferative and proinvasive mediators by ccRCC cells and might thus enhance metastatic colonization. Therefore, future studies aimed at developing specific inhibitory drugs of the Hippo signaling pathway or its downstream effectors described here seem warranted to generate novel therapeutic regimens against ccRCC.

Acknowledgments

We thank Miriam Menger, Nadine Fricker, and Martin Mahlberg for excellent technical assistance. The authors disclose no potential conflicts of interest.

References

[1] Rini BI, Campbell SC, and Escudier B (2009). Renal cell carcinoma. *Lancet* **373**, 1119–1132.

[2] Allory Y, Culine S, and de la Taille A (2011). Kidney cancer pathology in the new context of targeted therapy. *Pathobiology* **78**, 90–98.

[3] Dong J, Feldmann G, Huang J, Wu S, Zhang N, Comerford SA, Gayyed MF, Anders RA, Maitra A, and Pan D (2007). Elucidation of a universal size-control mechanism in *Drosophila* and mammals. *Cell* **130**, 1120–1133.

[4] Zeng Q and Hong W (2008). The emerging role of the hippo pathway in cell contact inhibition, organ size control, and cancer development in mammals. *Cancer Cell* **13**, 188–192.

[5] Steinhardt AA, Gayyed MF, Klein AP, Dong J, Maitra A, Pan D, Montgomery EA, and Anders RA (2008). Expression of Yes-associated protein in common solid tumors. *Hum Pathol* **39**, 1582–1589.

[6] Xu MZ, Yao TJ, Lee NP, Ng IO, Chan YT, Zender L, Lowe SW, Poon RT, and Luk JM (2009). Yes-associated protein is an independent prognostic marker in hepatocellular carcinoma. *Cancer* **115**, 4576–4585.

[7] Fernandez LA, Northcott PA, Dalton J, Fraga C, Ellison D, Angers S, Taylor MD, and Kenney AM (2009). YAP1 is amplified and up-regulated in hedgehog-associated medulloblastomas and mediates Sonic hedgehog-driven neural precursor proliferation. *Genes Dev* **23**, 2729–2741.

[8] Seliger B, Höhne A, Knuth A, Bernhard H, Ehring B, Tampé R, and Huber C (1996). Reduced membrane major histocompatibility complex class I density and stability in a subset of human renal cell carcinomas with low TAP and LMP expression. *Clin Cancer Res* **2**, 1427–1433.

[9] Trojaneck B, Niemitz S, Micka B, Lefterova P, Blasczyk R, Scheffold C, Huhn D, and Schmidt-Wolf IG (2000). Establishment and characterization of colon carcinoma and renal cell carcinoma primary cultures. *Cancer Biother Radiopharm* **15**, 169–174.

[10] Sievers E, Dreimuller P, Haferkamp A, Schmidt-Wolf IG, Buchler MW, Schmidt J, and Marten A (2007). Characterization of primary renal carcinoma cultures. *Urol Int* **79**, 235–243.

[11] van Kuppeveld FJ, van der Logt JT, Angulo AF, van Zoest MJ, Quint WG, Niesters HG, Galama JM, and Melchers WJ (1992). Genus- and species-specific identification of mycoplasmas by 16S rRNA amplification. *Appl Environ Microbiol* **58**, 2606–2615.

[12] Feldmann G, Dhara S, Fendrich V, Bedja D, Beaty R, Mullendore M, Karikari C, Alvarez H, Iacobuzio-Donahue C, and Jimeno A, et al (2007). Blockade of hedgehog signaling inhibits pancreatic cancer invasion and metastases: a new paradigm for combination therapy in solid cancers. *Cancer Res* **67**, 2187–2196.

[13] Haan C and Behrmann I (2007). A cost effective non-commercial ECL-solution for Western blot detections yielding strong signals and low background. *J Immunol Methods* **318**, 11–19.

[14] Tarca AL, Draghici S, Khatri P, Hassan SS, Mittal P, Kim JS, Kim CJ, Kusanovic JP, and Romero R (2009). A novel signaling pathway impact analysis. *Bioinformatics* **25**, 75–82.

[15] Livak KJ and Schmittgen TD (2001). Analysis of relative gene expression data using real-time quantitative PCR and the $2^{-\Delta\Delta CT}$ Method. *Methods* **25**, 402–408.

[16] Feldmann G, Mishra A, Bisht S, Karikari C, Garrido-Laguna I, Rasheed Z, Ottenhof NA, Dadon T, Alvarez H, and Fendrich V, et al (2011). Cyclin-dependent kinase inhibitor Dinaciclib (SCH727965) inhibits pancreatic cancer growth and progression in murine xenograft models. *Cancer Biol Ther* **12**, 598–609.

[17] Vogelstein B, Papadopoulos N, Velculescu VE, Zhou S, Diaz Jr LA, and Kinzler KW (2013). Cancer genome landscapes. *Science* **339**, 1546–1558.

[18] Roberts NJ, Vogelstein JT, Parmigiani G, Kinzler KW, Vogelstein B, and Velculescu VE (2012). The predictive capacity of personal genome sequencing. *Sci Transl Med* **4**, 133ra158.

[19] Matsuura K, Nakada C, Mashio M, Narimatsu T, Yoshimoto T, Tanigawa M, Tsukamoto Y, Hijiya N, Takeuchi I, and Nomura T, et al (2011). Downregulation of SAV1 plays a role in pathogenesis of high-grade clear cell renal cell carcinoma. *BMC Cancer* **11**, 523.

[20] Yoshimoto T, Matsuura K, Karnan S, Tagawa H, Nakada C, Tanigawa M, Tsukamoto Y, Uchida T, Kashima K, and Akizuki S, et al (2007). High-resolution analysis of DNA copy number alterations and gene expression in renal clear cell carcinoma. *J Pathol* **213**, 392–401.

[21] Girgis AH, Iakovlev VV, Beheshti B, Bayani J, Squire JA, Bui A, Mankaruos M, Youssef Y, Khalil B, and Khella H, et al (2012). Multilevel whole-genome analysis reveals candidate biomarkers in clear cell renal cell carcinoma. *Cancer Res* **72**, 5273–5284.

[22] Guo G, Gui Y, Gao S, Tang A, Hu X, Huang Y, Jia W, Li Z, He M, and Sun L, et al (2012). Frequent mutations of genes encoding ubiquitin-mediated proteolysis pathway components in clear cell renal cell carcinoma. *Nat Genet* **44**, 17–19.

[23] Dalgliesh GL, Furge K, Greenman C, Chen L, Bignell G, Butler A, Davies H, Edkins S, Hardy C, and Latimer C, et al (2010). Systematic sequencing of renal carcinoma reveals inactivation of histone modifying genes. *Nature* **463**, 360–363.

[24] Morris ZS and McClatchey AI (2009). Aberrant epithelial morphology and persistent epidermal growth factor receptor signaling in a mouse model of renal carcinoma. *Proc Natl Acad Sci U S A* **106**, 9767–9772.

[25] Habbig S, Bartram MP, Müller RU, Schwarz R, Andriopoulos N, Chen S, Sagmuller JG, Hoehne M, Burst V, and Liebau MC, et al (2011). NPHP4, a cilia-associated protein, negatively regulates the Hippo pathway. *J Cell Biol* **193**, 633–642.

[26] Habbig S, Bartram MP, Sägmüller JG, Griessmann A, Franke M, Müller RU, Schwarz R, Hoehne M, Bergmann C, and Tessmer C, et al (2012). The ciliopathy disease protein NPHP9 promotes nuclear delivery and activation of the oncogenic transcriptional regulator TAZ. *Hum Mol Genet* **21**, 5528–5538.

[27] Lamar JM, Stern P, Liu H, Schindler JW, Jiang ZG, and Hynes RO (2012). The Hippo pathway target, YAP, promotes metastasis through its TEAD-interaction domain. *Proc Natl Acad Sci U S A* **109**, E2441-2450.

[28] Perbal B (2001). NOV (nephroblastoma overexpressed) and the CCN family of genes: structural and functional issues. *Mol Pathol* **54**, 57–79.

[29] Chintalapudi MR, Markiewicz M, Kose N, Dammai V, Champion KJ, Hoda RS, Trojanowska M, and Hsu T (2008). Cyr61/CCN1 and CTGF/CCN2 mediate the proangiogenic activity of VHL-mutant renal carcinoma cells. *Carcinogenesis* **29**, 696–703.

[30] Schmitz P, Gerber U, Jüngel E, Schütze N, Blaheta R, and Bendas G (2013). Cyr61/CCN1 affects the integrin-mediated migration of prostate cancer cells (PC-3) in vitro. *Int J Clin Pharmacol Ther* **51**, 47–50.

[31] Zubac DP, Bostad L, Kihl B, Seidal T, Wentzel-Larsen T, and Haukaas SA (2009). The expression of thrombospondin-1 and p53 in clear cell renal cell carcinoma: its relationship to angiogenesis, cell proliferation and cancer specific survival. *J Urol* **182**, 2144–2149.

[32] Kohan DE, Cleland JG, Rubin LJ, Theodorescu D, and Barton M (2012). Clinical trials with endothelin receptor antagonists: what went wrong and where can we improve? *Life Sci* **91**, 528–539.

[33] Pflug BR, Zheng H, Udan MS, D'Antonio JM, Marshall FF, Brooks JD, and Nelson JB (2007). Endothelin-1 promotes cell survival in renal cell carcinoma through the ET_A receptor. *Cancer Lett* **246**, 139–148.

[34] Douglas ML, Richardson MM, and Nicol DL (2004). Endothelin axis expression is markedly different in the two main subtypes of renal cell carcinoma. *Cancer* **100**, 2118–2124.

[35] Groenewegen G, Walraven M, Vermaat J, de Gast B, Witteveen E, Giles R, Haanen J, and Voest E (2012). Targeting the endothelin axis with atrasentan, in combination with IFN-alpha, in metastatic renal cell carcinoma. *Br J Cancer* **106**, 284–289.

[36] Ling L, Maguire JJ, and Davenport AP (2013). Endothelin-2, the forgotten isoform: emerging role in the cardiovascular system, ovarian development, immunology and cancer. *Br J Pharmacol* **168**, 283–295.

[37] Ohkubo S, Ogi K, Hosoya M, Matsumoto H, Suzuki N, Kimura C, Ondo H, and Fujino M (1990). Specific expression of human endothelin-2 (ET-2) gene in a renal adenocarcinoma cell line. Molecular cloning of cDNA encoding the precursor of ET-2 and its characterization. *FEBS Lett* **274**, 136–140.

[38] Bot BM, Eckel-Passow JE, LeGrand SN, Hilton T, Cheville JC, Igel T, and Parker AS (2012). Expression of endothelin 2 and localized clear cell renal cell carcinoma. *Hum Pathol* **43**, 843–849.

[39] Grimshaw MJ, Hagemann T, Ayhan A, Gillett CE, Binder C, and Balkwill FR (2004). A role for endothelin-2 and its receptors in breast tumor cell invasion. *Cancer Res* **64**, 2461–2468.

[40] Hagemann T, Binder C, Binder L, Pukrop T, Trümper L, and Grimshaw MJ (2005). Expression of endothelins and their receptors promotes an invasive phenotype of breast tumor cells but is insufficient to induce invasion in benign cells. *DNA Cell Biol* **24**, 766–776.

[41] Said N, Smith S, Sanchez-Carbayo M, and Theodorescu D (2011). Tumor endothelin-1 enhances metastatic colonization of the lung in mouse xenograft models of bladder cancer. *J Clin Invest* **121**, 132–147.

[42] Tang SW, Chang WH, Su YC, Chen YC, Lai YH, Wu PT, Hsu CI, Lin WC, Lai MK, and Lin JY (2009). MYC pathway is activated in clear cell renal cell carcinoma and essential for proliferation of clear cell renal cell carcinoma cells. *Cancer Lett* **273**, 35–43.

[43] Fan Y, Liu Z, Fang X, Ge Z, Ge N, Jia Y, Sun P, Lou F, Bjorkholm M, and Gruber A, et al (2005). Differential expression of full-length telomerase reverse transcriptase mRNA and telomerase activity between normal and malignant renal tissues. *Clin Cancer Res* **11**, 4331–4337.

[44] Kozma L, Kiss I, Nagy A, Szakall S, and Ember I (1997). Investigation of c-myc and K-ras amplification in renal clear cell adenocarcinoma. *Cancer Lett* **111**, 127–131.

[45] Nelson J, Bagnato A, Battistini B, and Nisen P (2003). The endothelin axis: emerging role in cancer. *Nat Rev Cancer* **3**, 110–116.

[46] Khimji AK and Rockey DC (2010). Endothelin—biology and disease. *Cell Signal* **22**, 1615–1625.

[47] Shimazui T, Giroldi LA, Bringuier PP, Oosterwijk E, and Schalken JA (1996). Complex cadherin expression in renal cell carcinoma. *Cancer Res* **56**, 3234–3237.

[48] Katagiri A, Watanabe R, and Tomita Y (1995). E-cadherin expression in renal cell cancer and its significance in metastasis and survival. *Br J Cancer* **71**, 376–379.

[49] Shimazui T, Yoshikawa K, Uemura H, Hirao Y, Saga S, and Akaza H (2004). The level of cadherin-6 mRNA in peripheral blood is associated with the site of metastasis and with the subsequent occurrence of metastases in renal cell carcinoma. *Cancer* **101**, 963–968.

[50] Li G, Passebosc-Faure K, Gentil-Perret A, Lambert C, Genin C, and Tostain J (2005). Cadherin-6 gene expression in conventional renal cell carcinoma: a useful marker to detect circulating tumor cells. *Anticancer Res* **25**, 377–381.

[51] Creighton CJ, Morgan M, Gunaratne PH, Wheeler DA, Gibbs RA, Gordon Robertson A, Chu A, Beroukhim R, Cibulskis K, and Signoretti S, et al (2013). Comprehensive molecular characterization of clear cell renal cell carcinoma. *Nature* **499**, 43–49.

[52] Dey N, Das F, Ghosh-Choudhury N, Mandal CC, Parekh DJ, Block K, Kasinath BS, Abboud HE, and Choudhury GG (2012). microRNA-21 governs TORC1 activation in renal cancer cell proliferation and invasion. *PLoS One* **7**, e37366.